Direct silylation of a mesostructured precursor for novel mesoporous silica KSW-2

ARTICLE *in* LANGMUIR · SEPTEMBER 2002

Impact Factor: 4.46 · DOI: 10.1021/la020543h

4 AUTHORS, INCLUDING:

Tatsuo Kimura
National Institute of Advanced Industrial Sci…
82 PUBLICATIONS **1,811** CITATIONS

Direct Silylation of a Mesostructured Precursor for Novel Mesoporous Silica KSW-2

Tetsuro Shigeno,[†] Masatsune Nagao,[†] Tatsuo Kimura,[‡] and Kazuyuki Kuroda*[,†,§]

Department of Applied Chemistry, Waseda University, Ohkubo-3, Shinjuku-ku, Tokyo 169-8555, Japan, National Institute of Advanced Industrial Science and Technology (AIST), Ceramics Research Institute, Shimoshidami, Moriyama-ku, Nagoya 463-8560, Japan, and Kagami Memorial Laboratory for Materials Science and Technology, Waseda University, Nishiwaseda 2-8-26, Shinjuku-ku, Tokyo 169-0051, Japan

Received June 12, 2002

A mesostructured precursor for KSW-2 with semi-squared mesopores was directly modified with chlorotrimethylsilane and chlorooctyldimethylsilane for the first time. The silylated products were characterized by powder XRD, IR, ^{29}Si MAS NMR, CHN analysis, and N_2 and water vapor adsorption measurements. Mesoporous silica KSW-2 prepared by calcination of the precursor was also silylated in a similar manner. The mesostructures of the precursor and of KSW-2 were retained after silylation. The characteristics of semi-squared mesopores remarkably changed; the hydrophobicity of the derivatives increased substantially after silylation. The BET surface area, the pore volume, and the width of the semi-squared mesopores decreased after silylation, and the degree of the decrease is larger for the octyldimethylsilyl derivatives than that for the trimethylsilyl derivatives. The numbers of the silyl groups grafted on the directly silylated derivatives are larger than those on the silylated KSW-2. In addition, calcination of the trimethylsilylated products yielded mesoporous silica with the same structure in which the pore wall thickness was increased because of the participation of the silyl groups to the silica network by oxidation.

Introduction

Much attention has been paid to the synthesis of ordered mesoporous silicas with high surface areas as well as their applications to catalysts, catalyst supports, adsorbents, inclusion vessels, optical and electronic devices, etc.[1−5] Various morphologies of mesoporous silica (such as fibers, films, and spheres) have been extensively studied because of their scientific and technological importance.

Recently, we reported the formation of novel mesoporous silica (denoted as KSW-2) by mild acid treatment of a layered aklyltrimethylammonium (C_nTMA)−kanemite complex.[6,7] Being different from hexagonal mesoporous silica (FSM-16) derived from kanemite,[2,3] KSW-2 has an orthorhombic structure with rectangular arrangements of semi-squared one-dimensional channels that have not been found previously because the shapes of all the other ordered mesopores have been governed by those of organic assemblies as structure directing agents.[8,9] Therefore, KSW-2 is quite unique and has stimulated the development of ordered mesoporous materials. The mesostructured precursor of KSW-2 is formed through the bending of individual silicate sheets of kanemite.[6] Kanemite is a layered silicate composed of single sheets that are made up with SiO_4 tetrahedral units.[10] Consequently, the structural unit of the silicate sheet in kanemite is retained in the precursor to some extent, although the regularity is reduced after calcination.[6]

One of the most important features of mesoporous silica is the presence of silanol groups (Si−OH) on the inner surfaces, and the Si−OH groups can be modified in various ways. Ordered mesoporous silica has been organically modified by grafting, coating, and co-condensation methods.[11] Among them, grafting by post-treatment with reactive reagents is used most frequently. Typical reactions include silylation[12,13] (eq 1), esterification[14] with alcohols (eq 2), and functionalization

* Corresponding author e-mail: kuroda@waseda.jp.
† Department of Applied Chemistry, Waseda University.
‡ National Institute of Advanced Industrial Science and Technology (AIST), Ceramics Research Institute.
§ Kagami Memorial Laboratory for Materials Science and Technology, Waseda University.

(1) Yanagisawa, T.; Shimizu, T.; Kuroda, K.; Kato, C. *Bull. Chem. Soc. Jpn.* **1990**, 63, 988−992.
(2) Inagaki, S.; Fukushima, Y.; Kuroda, K. *J. Chem. Soc., Chem. Commun.* **1993**, 680−682.
(3) Inagaki, S.; Koiwai, A.; Suzuki, N.; Fukushima, Y.; Kuroda, K. *Bull. Chem. Soc. Jpn.* **1996**, 69, 1449−1457.
(4) Kresge, C. T.; Leonowicz, M. E.; Roth, W. J.; Vartuli, J. C.; Beck, J. S. *Nature* **1992**, 359, 710−712.
(5) Beck, J. S.; Vartuli, J. C.; Roth, W. J.; Leonowicz, M. E.; Kresge, C. T.; Schmitt, K. D.; Chu, C. T.-W.; Olson, D. H.; Sheppard, E. W.; McCullen, S. B.; Higgins, J. B.; Schlenker, J. L. *J. Am. Chem. Soc.* **1992**, 114, 10834−10843.
(6) Kimura, T.; Kamata, T.; Fuziwara, M.; Takano, Y.; Kaneda, M.; Sakamoto, Y.; Terasaki, O.; Sugahara, Y.; Kuroda, K. *Angew. Chem., Int. Ed.* **2000**, 39, 3855−3859.
(7) Kimura, T.; Itoh, D.; Okazaki, N.; Kaneda, M.; Sakamoto, Y.; Terasaki, O.; Sugahara, Y.; Kuroda, K. *Langmuir* **2000**, 16, 7624−7628.
(8) Monnier, A.; Schüth, F.; Huo, Q.; Kumar, D.; Margolese, D.; Maxwell, R. S.; Stucky, G. D.; Krishnamurty, M.; Petroff, P.; Firouzi, A.; Janicke, M.; Chmelka, B. F. *Science* **1993,** 261, 1299−1303.
(9) Huo, Q.; Margolese, D. I.; Ciesla, U.; Demuth, D. G.; Feng, P.; Gier, T. E.; Sieger, P.; Firouzi, A.; Chmelka, B. F.; Schüth, F.; Stucky, G. D. *Chem. Mater.* 1**994,** 6, 1176−1191.
(10) Vortmann, S.; Rius, J.; Marler, B.; Gies, H. *Eur. J. Mineral.* **1999**, *11*, 125−134.
(11) Stein, A.; Melde, B. J.; Schroden, R. C. *Adv. Mater.* **2000**, *12*, 1403−1419.
(12) Yanagisawa, T.; Shimizu, T.; Kuroda, K.; Kato, C. *Bull. Chem. Soc. Jpn.* **1990**, *63*, 1535−1537.
(13) Kimura, T.; Saeki, S.; Sugahara, Y.; Kuroda, K. *Langmuir* **1999**, *15*, 2794−2798.
(14) Kimura, T.; Kuroda, K.; Sugahara, Y.; Kuroda, K. *J. Porous Mater.* **1998**, *5*, 127−132.

10.1021/la020543h CCC: $22.00
Published on Web 09/06/2002

with Grignardreagents[15] (eq 3):

$$\equiv Si{-}OH + R_3Si{-}Cl \rightarrow \equiv Si{-}O{-}SiR_3 + HCl \quad (1)$$

$$\equiv Si{-}OH + R{-}OH \rightarrow \equiv Si{-}O{-}R + H_2O \quad (2)$$

$$\equiv Si{-}OH + R{-}OH \rightarrow \equiv Si{-}O{-}R, \equiv Si{-}O{-}R + RMgX \rightarrow \equiv Si{-}R \quad (3)$$

Consequently, the material systems can be extended to a wide variety of organic silicate mesostructured materials.[16] Organic modification of ordered mesoporous silica is very effective to control pore size, and it improves the mechanical strength and tailors the surface functionality.[5,12,13,17−23] Trimethylsilylation of ordered mesoporous silica has been reported since the beginning of the research on ordered mesoporous materials.[5,12] Recent advances include the removal of toxic heavy metal ions, polymer syntheses in a confined space, optical resolution of racemic mixtures, and immobilization of biological molecules.[11,24]

In contrast to conventional mesoporous silicas composed of amorphous silica walls, the mesostructured precursor of KSW-2 possesses the silicate units originated from kanemite in the wall to some extent.[6] It is interesting that the wall structure of the precursor is composed of partly intralayer-condensed individual silicate sheets in kanemite.[6] Nevertheless, the ordering of the wall structure was reduced during calcination to remove organic fractions. Therefore, in this study, a mesostructured precursor of KSW-2 was directly modified with silylating agents on the presumption that the wall might have some regularities after the modification. KSW-2 was also silylated for comparison, and the adsorption characteristics of these materials are presented.

Experimental Section

Synthesis of a Mesostructured Precursor for Novel Mesoporous Silica KSW-2. An aqueous solution of NaOH was added to high-quality water glass to prepare a solution with the Na:Si ratio of 1.0.[6] The solution was dried and heated at 750 °C for 1 h in air, which results in the formation of δ-$Na_2Si_2O_5$ after cooling. One gram of δ-$Na_2Si_2O_5$ was pulverized and dispersed in 50 mL of distilled water, and the suspension was stirred at room temperature for 30 min. The product (kanemite, $NaHSi_2O_5 \cdot 3H_2O$) was centrifuged and used for further reactions without air-drying. The purity of air-dried kanemite was checked by powder XRD, and the ^{29}Si MAS NMR spectrum of kanemite showed only one peak attributed to Q^3 environment (O−Si(−O−Si≡)$_3$).[10] A layered C_{16}TMA−kanemite complex was prepared by mixing kanemite and an aqueous solution of C_{16}TMACl (0.1 M) at room temperature for 3 days, where the C_{16}TMA:Si molar ratio was 2.0. The resulting layered C_{16}TMA−kanemite complex was dispersed in distilled water. The pH value of this suspension was decreased down to 5.5 by the addition of 1 M acetic acid for 30 min. Mesoporous silica KSW-2 was also prepared for comparison. The mesostructured precursor was air-dried and calcined at 550 °C at a heating rate of 5 °C/min in ambient air for 6 h to remove organic fractions.

Silylation of the Precursor. Chlorotrimethylsilane (TMS-Cl) and octyldimethylchlorosilane (ODMS-Cl), both of which were purchased from Tokyo Kasei Co., were used without further purification. The mesostructured precursor was preheated at 150 °C for 3 h under vacuum. After 1 g of the precursor was dispersed in 50 mL of toluene, 10 mL of the silylating agent (TMS-Cl or ODMS-Cl) was added to the mixture. The suspension was refluxed for 24 h in the presence of 5 mL of pyridine under N_2 atmosphere. Pyridine was used as an agent both to promote the direct reaction of the chlorosilyl groups with the surface hydroxyl groups as a catalyst[25] and to trap excess hydrogen chloride generated during the reaction. The degree of silylation was slightly decreased when pyridine was not added. The products were air-dried after being washed with toluene and ethanol. Silylation of KSW-2 was also carried out in a similar manner. To examine whether the silyl groups can be used to cover the surface of the mesopores of KSW-2, trimethylsilylated KSW-2 (TMS-KSW-2) and trimethylsilylated precursor (TMS-precursor) were calcined at 550 °C at a heating rate of 5 °C/min in ambient air for 6 h to remove the methyl groups.

Characterization. Powder XRD patterns were obtained by using a Mac Science M03XHF^{22} diffractometer with monochromated Fe Kα radiation for the measurement of low angle regions and a Mac Science MXP^3 diffractometer with monochromated Cu Kα radiation for higher angles. IR spectra were recorded on a Perkin-Elmer FT−IR Spectrum One spectrometer by the KBr disk technique after samples were dehydrated at 120 °C. Nitrogen adsorption and desorption isotherms were obtained by using a BELSORP 28 apparatus (Bel Japan, Inc.) at 77 K. Samples were heated at 120 °C for 3 h to a residual pressure of 1.3 Pa (10^{-2} Torr) prior to the measurements. Specific surface areas were determined by the BET method using the data before Kelvin condensation. Because the shape of the mesopores is almost squared, the width of the pore was determined by the equation of $4V/S$, where V is the pore volume and S is the inner surface area, which is the most reliable estimation of the pore size in this case. Inner surface area was calculated by the subtraction of outer surface area by a *t*-plot method from total BET surface area. The hydrophobic nature of the silylated derivatives was examined by water vapor adsorption measurements. Water adsorption isotherms were obtained by using a BELSORP 18 apparatus (Bel Japan, Inc.) at 298 K. Thermogravimetry and differential thermal analysis (TG−DTA) were performed by a Mac Science 2000S apparatus with a heating rate of 10 °C/min in an air flow. CHN analysis was conducted with a Perkin-Elmer PE2400II instrument. Solid-state ^{29}Si MAS NMR measurements were performed on a JEOL JNM CMX-400 spectrometer at a spinning rate of 5 kHz and a resonance frequency of 79.30 MHz with a 45° pulse length of 4.1 μs and a recycle time of 100 s. This recycle time has been proven to be long enough to permit complete relaxation of the Si nucleus, based on our previous measurements. The chemical shift was expressed with respect to tetramethylsilane. Intensity ratios of the signals in the ^{29}Si spectra were calculated after deconvolution of the peaks by the use of a MacFID simulation program.

Results and Discussion

Characterization of a Mesostructured Precursor and the Calcined Product (KSW-2). A mesostructured precursor of KSW-2 was prepared by mild acid treatment of a layered C_{16}TMA−kanemite complex.[6] The XRD pattern of the mesostructured precursor is shown in Figure 1. All the XRD peaks in low angles are assignable to an orthorhombic structure ($d_{110} = 4.1$ nm). In addition, broad peaks containing a peak at the *d*-spacing of 0.37 nm were observed in the range of 15−30°. This observation indicates that the structural units in kanemite were retained in

(15) Yamamoto, K.; Tatsumi, T. *Microporous Mesoporous Mater.* **2001**, *44*−*45*, 459−464.
(16) Sayari, A.; Hamoudi, S. *Chem. Mater.* **2001**, *13*, 3151−3168.
(17) Tatsumi, T.; Koyano, K. A.; Tanaka, Y.; Nakata, S. *Chem. Lett.* **1997**, 469−470.
(18) Tatsumi, T.; Koyano, K. A.; Tanaka, Y.; Nakata, S. *J. Porous Mater.* **1999**, *6*, 13−17.
(19) Ishikawa, T.; Matsuda, M.; Yasukawa, A.; Kandori, K.; Inagaki, S.; Fukushima, T.; Kondo, S. *J. Chem. Soc., Faraday Trans.* **1996**, *92*, 1985−1989.
(20) Antochshuk, V.; Jaroniec, M. *Chem. Mater.* **2000**, *12*, 2496−2501.
(21) Wouters, B. H.; Chen, T. H.; Dewilde, M.; Grobet, P. J. *Microporous Mesoporous Mater.* **2001**, *44*, 453−457.
(22) Zhao, X. S.; Lu, G. Q.; Hu, X. *Microporous Mesoporous Mater.* **2000**, *41*, 37−47.
(23) Impens, N. R. E. N.; van der Voort, P.; Vansant, E. F. *Microporous Mesoporous Mater.* **1999**, *28*, 217−232.
(24) Price, P. M.; Clark, J. H.; Macquarrie, D. J. *J. Chem. Soc., Dalton Trans.* **2000**, *2*, 101−110.
(25) Tripp, C. P.; Hair, M. L. *J. Phys. Chem.* **1993**, *97*, 5693−5698.

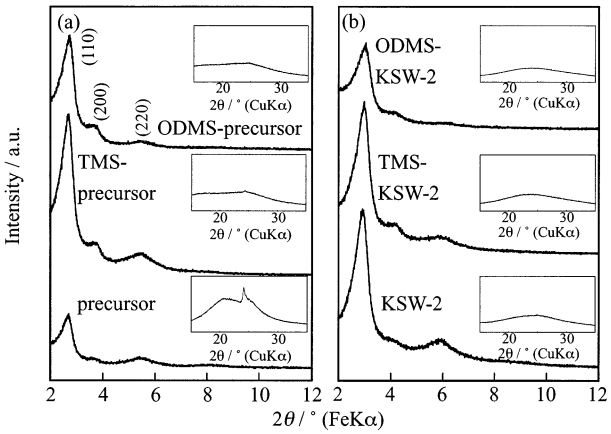

Figure 1. XRD patterns of (a) precursor and the silylated derivatives and (b) KSW-2 and the silylated derivatives.

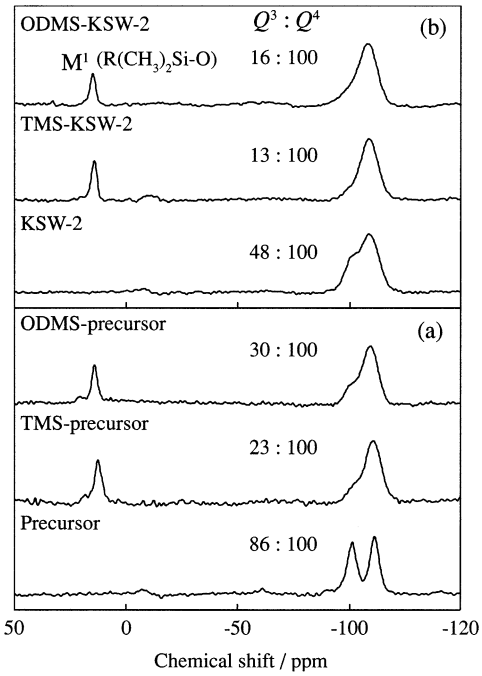

Figure 2. ^{29}Si MAS NMR spectra of (a) precursor and the silylated derivatives and (b) KSW-2 and the silylated derivatives.

the mesostructured precursor to some extent, as reported previously.[6] This is one of the most interesting characters of novel mesoporous silica KSW-2 derived from kanemite. The broad XRD peaks were further broadened after calcination, indicating the transformation to a less ordered local structure. Nevertheless, the mesostructure did not change ($d_{110} = 3.8$ nm), and the peak intensities increased because of no scattering due to the surfactants (Figure 1).

The density of silanol (Si−OH) groups at the surface of KSW-2 was calculated by using the data of N_2 adsorption and ^{29}Si MAS NMR measurements. The BET surface area of KSW-2 was 1190 m^2 g^{-1}. The ^{29}Si MAS NMR spectra of the precursor and KSW-2 are shown in Figure 2. The peaks due to Q^3 (OSi(O−Si≡)$_3$) and Q^4 (Si(O−Si≡)$_4$) environments were observed at around −101 and −110 ppm, respectively. The Q^3 and Q^4 intensity ratios are also shown in the figure. The ratio decreased during calcination, meaning the condensation of the Q^3 sites in the precursor and a shrinkage of the network. Because the Si atoms of KSW-2 consist of only Q^3 and Q^4 environments, the density of the Si−OH groups can be calculated on the basis of the Q^3 and Q^4 intensity ratios of KSW-2 (Figure 2b bottom) and on the specific surface area, supposing that all Q^3 sites are due to Si−OH groups. The density was estimated to be 2.8 groups nm^{-2}. It is quite difficult to estimate the density of the Si−OH groups in the precursor by the same manner because the specific surface area cannot be determined. In addition, Si−O$^-$ sites (associated with the surfactants) are present in the precursor. Therefore, the total density of both the Si−OH groups and the Si−O$^-$ sites was roughly estimated on the basis of the Q^3 and Q^4 intensity ratio of the precursor (86:100), being about 1.8 times larger than that of KSW-2. Consequently, the total density of both the Si−OH groups and the Si−O$^-$ sites in the precursor is calculated to be approximately 5 groups nm^{-2}.

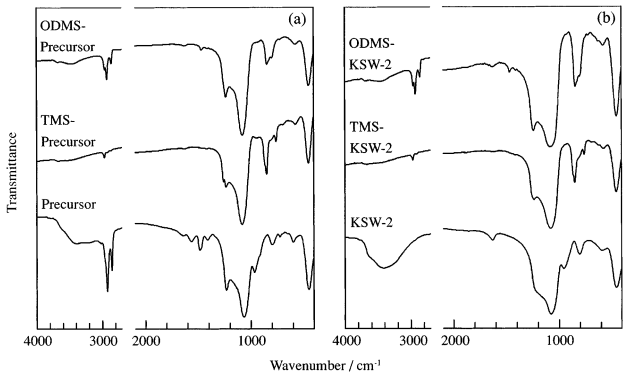

Figure 3. IR spectra of (a) precursor and the silylated derivatives and (b) KSW-2 and the silylated derivatives.

The unique character of the precursor is that it retains the original silicate framework to some extent. In addition, the precursor has a larger amount of Si−OH groups than KSW-2, indicating less condensation of the network. Therefore, silylation of the precursor can be a way to synthesize organically modified mesoporous silica retaining the original silicate units at least partly.

Silylation of the Precursor. The XRD patterns of the silylated products (Figure 1) showed the retention of the mesostructure of the precursor. There were basically no significant changes in the 2θ range between 2 and 12° in the XRD patterns of the precursor after the reactions with TMS-Cl and ODMS-Cl. The main peaks due to d_{110} were unchanged (TMS-precursor; 4.1−4.1 nm, ODMS-precursor; 4.1−4.0 nm). The TEM image of the TMS-precursor showed that semi-squared mesopores are observed clearly (Figure A in Supporting Information) and that their periodic distance of adjacent pores is in good agreement with the value from the XRD data (ca. 3.9 nm). These results indicate that the original mesostructure was retained.

In the IR spectra of the precursor and the silylated products (Figure 3), the spectrum of the TMS-precursor showed the absorption bands attributed to TMS groups at 1257 (δ_s SiCH$_3$), 848 (γ Si(CH$_3$)$_3$), and 758 cm^{-1} (γ Si-(CH$_3$)$_3$). As for the ODMS-precursor, the absorption bands attributed to ODMS groups were observed at 2959 (ν_{as} CH$_3$), 2926 (ν_{as} CH$_2$), 2857 (ν_s CH$_2$), 1255 (δ_s SiCH$_3$), and 846 cm^{-1} (γ Si(CH$_3$)$_2$). The ^{29}Si MAS NMR spectra of the TMS- and ODMS-precursors are shown in Figure 2a. The intense Q^4 peaks (−110 ppm) with shoulder Q^3 signals (−101 ppm) were detected, and the M^1 peaks due to the silyl groups (R$_3$Si−O−Si≡) newly appeared at 14 ppm. The presence of the M^1 peaks and the substantial decrease in the Q^3 signals in the spectra indicate the successful silylation. All of these results strongly support that TMS and ODMS groups have attached to the precursor.

On the other hand, the characteristic bands due to C$_{16}$-TMA cations at 1408 (δ NH$_4^+$), which are observed for the

Table 1. Characteristics of Mesoporous Silica KSW-2 and the Silylated Derivatives

	BET surface area ($m^2\ g^{-1}$)	pore volume ($mL\ g^{-1}$)	width of pore[a] (nm)	carbon content (wt %)	nitrogen content (wt %)	no.of silyl groups per 1 mol of SiO_2
KSW-2	1190	0.60	2.7			
TMS-precursor	800	0.31	2.2	12.7	0.06	0.25
TMS-KSW-2	770	0.29	2.1	9.2	0.06	0.17
ODMS-precursor	470	0.12	1.6	25.6	0.09	0.17
ODMS-KSW-2	430	0.10	1.5	21.5	0.08	0.14
calcined TMS-precursor	1110	0.48	2.3			
calcined TMS-KSW-2	1000	0.40	2.1			

[a] The width of pore was determined by the equation of $4V/S$, where V is pore volume and S is inner surface area.

precursor, disappeared after silylation. This result indicates that the surfactants were virtually removed during trimethylsilylation. The almost complete removal of C_{16}-TMA cations during silylation was also proven by CHN analysis (Table 1). Nitrogen contents due to C_{16}TMA cations were negligibly small in both of the derivatives (<0.1 mass %). The removal of surfactants can be explained by ion-exchange reactions of C_{16}TMA cations with protons formed by silylation.[26]

The degree of grafting for the precursor is estimated by using the number of silyl groups per SiO_2 (Table 1) because the surface area of the precursor cannot be determined. The numbers of the silyl groups per 1 mol SiO_2 for the silylated precursors were calculated to be 0.25 for TMS and 0.17 for ODMS by using both CHN and TG data. The higher grafting ratio of TMS groups is possibly due to the lower occupying area and lower steric hindrance.

Silylation of Calcined KSW-2. KSW-2 was also silylated with TMS-Cl and ODMS-Cl. As was found for the silylated precursors, the XRD patterns of the silylated KSW-2 (Figure 1) also showed the retention of the mesostructure. The main peaks due to d_{110} were 3.7 nm for TMS-KSW-2 (d_{110} = 3.8 nm before silylation) and 3.7 nm for ODMS-KSW-2 (d_{110} = 3.7 nm before silylation).

The ^{29}Si MAS NMR spectra of TMS- and ODMS-KSW-2 are shown in Figure 2b. In addition to the intense Q^4 peaks (−110 ppm) with shoulder Q^3 peaks (−101 ppm), the M^1 peaks due to the silyl groups were observed at 14 ppm. The result indicates that the successful silylation of KSW-2 was also achieved by the same procedure. On the basis of the carbon contents, the grafted numbers of TMS and ODMS groups on the surface of KSW-2 were 1.6 and 1.3 groups nm^{-2}, respectively. These values are equivalent to 0.17 TMS groups/SiO_2 and 0.14 ODMS groups/SiO_2, being smaller than those for the silylated precursors (0.25 for TMS and 0.17 for ODMS). This is quite reasonable because KSW-2 has less Si−OH groups than the precursor.

Compared to the TMS system, a larger amount of silanol groups remained in the ODMS system, as was discussed for the silylated precursors. The amounts of TMS and ODMS groups grafted on FSM-type mesoporous silica are 1.7 and 1.3 groups nm^{-2}, respectively.[13] Therefore, the packing densities of the silyl groups on the surfaces are almost similar in these two mesoporous silicas derived from kanemite.

Local Structures of the Precursor and KSW-2 after Silylation. The mesostructures of the precursor and KSW-2 did not change during the silylation as described above, and organically modified mesoporous silica with a novel mesostructure (semi-square mesopores) was obtained by direct silylation. All the N_2 adsorption isotherms of KSW-2 and the TMS derivatives from both the precursor and the KSW-2 showed a type IV behavior characteristic

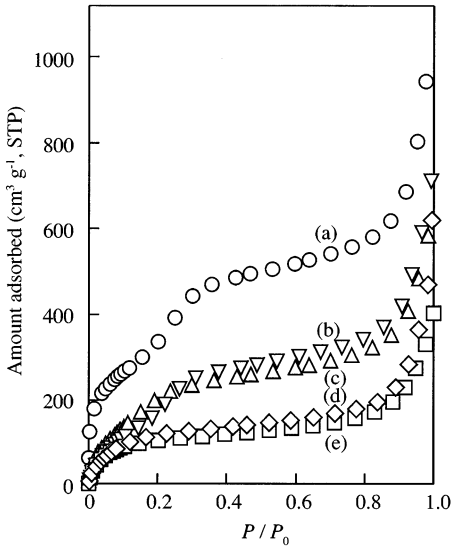

Figure 4. Nitrogen adsorption isotherms of (a) KSW-2 (○), (b) TMS-precursor (▽), (c) TMS-KSW-2 (△), (d) ODMS-precursor (◇), and (e) ODMS-KSW-2 (□).

of mesoporous materials, while type I-like isotherms were observed for the ODMS derivatives (Figure 4). The BET surface areas, the pore volumes, and the widths of the square mesopores are listed in Table 1. The BET surface area, the pore volume, and the width of the pore were decreased for all the silylated samples. These changes correlate with the size of the silyl groups. Because the ODMS group is bulkier than the TMS group, these parameters for the ODMS derivatives are lower than those for the TMS derivatives. Silylated precursors show slightly larger values on the mesoporosity than silylated KSW-2 both in the TMS and in the ODMS derivatives, which should be attributable to the less condensed structure of the precursor. This is consistent with the larger lattice constants of the precursor and suggests that the derivatives should have the structural units of the original framework of the starting material.

However, the peak at the d-spacing of 0.37 nm (found in the pattern of the precursor) became very broad through silylation, suggesting that the capping induced the variation of the local arrangement of the silicate framework. We have recently succeeded in synthesizing organic derivatives of a layered C_{16}TMA−kanemite by monochloroalkyldimethyl-, dichloroalkylmethyl-, and trichloroalkylsilanes and found that the structural variations are diverse, depending on the kind of the silylating reagent and the alkyl chain length.[27] Therefore, silylation of the mesostructured precursor of KSW-2 under milder conditions and by using bifunctional and trifunctional silylating reagents would also be interesting for further silylation.

(26) Yanagisawa, T.; Kuroda, K.; Kato, C. *React. Solids* **1988**, *5*, 167−175.

(27) Shimojima, A.; Mochizuki, D.; Kuroda, K. *Chem. Mater.* **2001**, *13*, 3603−3609.

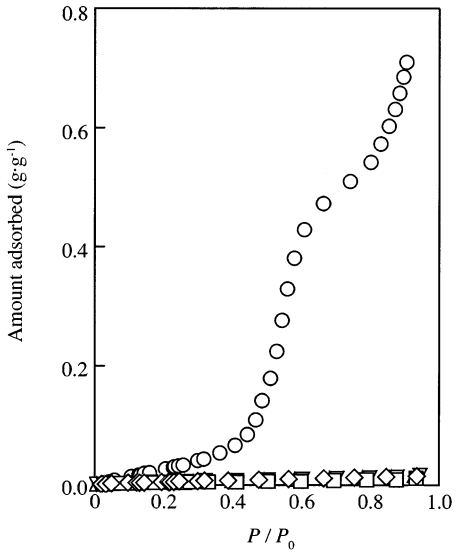

Figure 5. Adsorption isotherms of water vapor on KSW-2 (○), TMS-precursor (▽), TMS-KSW-2 (△), ODMS-precursor (◇), and ODMS-KSW-2 (□).

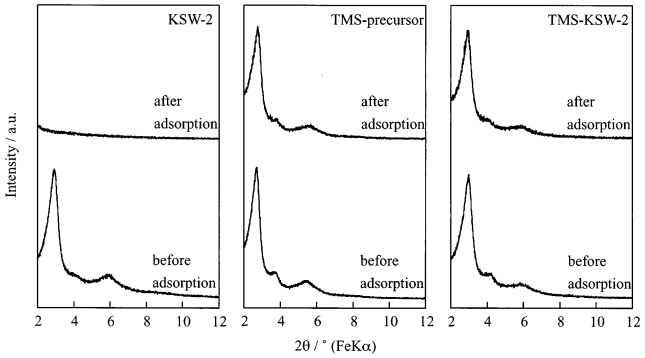

Figure 6. Changes in XRD patterns of KSW-2, TMS-precursor, and TMS-KSW-2 by water vapor adsorption.

Properties of the Silylated Derivatives. The water vapor adsorption isotherms of KSW-2 and the silylated derivatives from both precursor and KSW-2 are shown in Figure 5. The isotherm of KSW-2 showed a type V behavior, indicating weak interactions between the surface of KSW-2 and water molecules. The amounts of adsorbed water for the silylated derivatives were much smaller than that observed for KSW-2. The silylated derivatives equally displayed their hydrophobic behavior. Though the grafted number of the silyl groups on TMS-KSW-2 was larger than that on ODMS-KSW-2, there were no appreciable differences between them. All the data indicate that the hydrophobicity of KSW-2 was drastically increased by silylation.

The XRD patterns of KSW-2 and the TMS derivatives from both precursor and KSW-2 before and after the adsorption of water vapor are shown in Figure 6. The XRD pattern of KSW-2 after the adsorption did not exhibit any distinct peaks, indicating a structural collapse. On the other hand, the XRD patterns of the silylated derivatives did not change after the adsorption. The increased hydrophobicity of the silylated derivatives improved the stability against water vapor. It has been reported that the stability of MCM-41 materials against the treatment with water depends on the nature of pore walls. The instability in the presence of water is explained by the hydrolysis of Si−O−Si bonds.[19,28] Accordingly, the

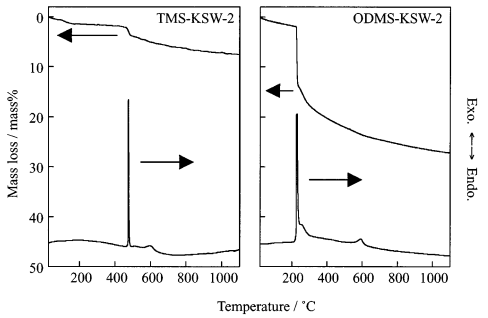

Figure 7. TG−DTA curves of silylated derivatives derived from KSW-2.

increased stability presented here is attributed to the formation of Si−OSiR$_3$ linkage on the inner surfaces.

The TG-DTA curve of TMS-KSW-2 (Figure 7) showed a sharp exothermic peak at 475 °C and a weak and broad exothermic peak at around 595 °C. The sharp peak is ascribed to the oxidative decomposition of TMS groups, while the weak peak may be assigned to the combustion of remaining carbon species. On the other hand, ODMS-KSW-2 showed a sharp peak at 228 °C with a shoulder centered at 252 °C and a weak broad peak at around 592 °C. The peak at the relatively lower temperature is due to the combustion of octyl groups. The presence of the exothermic peaks strongly supports the silylation, and it should also be noted that the peaks appeared at relatively high temperature for the TMS derivatives.

Trimethylsilylated products of the precursor and KSW-2 were calcined to find the possibility of tuning the pore size. After calcination of TMS-precursor and TMS-KSW-2, the main peaks due to d_{110} were very slightly shifted to higher angles in the XRD patterns. As shown in Table 1, the BET surface areas and pore volumes were larger than those of the corresponding silylated derivatives and lower than that of KSW-2, while the width of the pores was reduced from 2.7 nm (KSW-2) to 2.3 and 2.1 nm for the calcined TMS-precursor and TMS-KSW-2, respectively. These results indicate that the pores of the calcined TMS derivatives were partly covered with silica that was formed by oxidation of attached TMS groups. Because the lattice constants of the *a* and *b* axes of KSW-2 are very similar, the average value can be calculated from the d_{110} value of KSW-2 by assuming the lattice is square. On the basis of d_{110} (Figure 1), the *a* parameter was estimated to be 3.8 nm. From the N_2 adsorption data of KSW-2, the width of the square mesopore was estimated to be 2.7 nm. Consequently, the wall thickness of KSW-2 was evaluated to be approximately 1.1 nm. On the other hand, the wall thicknesses of both calcined TMS-KSW-2 and calcined TMS-precursor were approximately 1.6 nm by assuming the retention of the structure. Therefore, the wall was thickened by calcining silylated derivatives, confirming an additional role of silyl groups to control the structure of the pore wall of mesoporous silica derived from the single layered polysilicate.

Conclusions

Mesoporous silica KSW-2 and the precursor are silylated by the reaction with chlorotrimethylsilane and octyldimethlchlorosilane without the collapse of the mesostructures. The semi-squared mesopores found only for KSW-2 and the precursor are retained after silylation. The grafted numbers for the silylated derivatives derived

(28) Koyano, K. A.; Tatsumi, T.; Tanaka, Y.; Nakata, S. *J. Phys. Chem. B* **1997**, *101*, 9436−9440.

from the precursor are larger than those from KSW-2. All the silylated derivatives show lower values of BET surface area, pore volume, and width of the mesopore than those for KSW-2, and the values for ODMS derivatives are lower than those for TMS derivatives because of the steric hindrance. The hydrophobicity and the stability against water vapor significantly increase by silylation. The calcined products of the silylated derivatives have shorter widths of the mesopores than KSW-2. The wall thickness and the width of the pore of KSW-2 can be tunable if silylating agents are properly chosen. Therefore, the present results suggest possible molecular design based on this mesoporous silica. Novel silica organic hybrids are obtained by silylation of mesoporous silica KSW-2 and the precursor. Because KSW-2 has a very unique shape of mesopores, the organic derivatives should afford distinctive characteristics such as specific reaction media and adsorption sites that other mesoporous silicas cannot provide. Although the regularity of the silicate framework retained in the precursor was not found for the silylated derivatives by powder XRD, there should be some ordering in the framework because restructuring of the skeleton cannot occur during the silylation. Further research is required toward the construction of organically modified mesoporous silicas with retaining a higher ordered silica network close to the original structure, which would be realized under milder reaction conditions by using well-designed reagents.

Acknowledgment. This work was partially supported by a Grant-in-Aid for COE research, Ministry of Education, Culture, Sports, Science and Technology (MEXT), Japan.

Supporting Information Available: Figure A. This material is available free of charge via the Internet at http://pubs.acs.org.

LA020543H